Chromatography of Nonadsorbable Gases

RAMON L. CERRO and J. M. SMITH

University of California, Davis, California

Chromatographic techniques are used with nonadsorbable and slightly adsorbable tracers to evaluate mass transfer parameters in packed beds. If accurate values of intraparticle diffusivities are to be obtained, it appears that long beds of relatively large particles must be used. Otherwise the moments of the chromatographic peaks are too small for accurate analysis. With adsorbable gases, such precautions are not necessary, and, in addition, the adsorption rate constant can be estimated. However, the intraparticle diffusivity determined for adsorbable gases can include a contribution due to surface migration. The method is applicable to all types of porous particles used as catalysts or catalyst carriers.

A combination of measurements of slightly adsorbable and nonabsorbable tracers can be used to approximate the adsorption rate constant for a slightly adsorbable gas such as nitrogen.

Chromatography offers a new method for measuring transport parameters in packed beds, especially intraparticle diffusivity. The method is rapid and versatile. Recent mathematical solutions (*1* to *3*) for the partial differential equations describing the concentration of the tracer component provide a clear interpretation in terms of the basic transport steps. The Kubin theory (*1, 2*) has been used with an adsorbable tracer to evaluate the mass transfer rate constants of hydrocarbons in beds of silica gel (*4, 5*), and to study thermal and nonlinear effects (*6*). Recently, Davis and Scott (*10*) have shown that the chromatographic technique can be employed with a nonadsorbable tracer to obtain intraparticle diffusivities. Their analysis was developed from the modified plate (or rate) theory (*7* to *11*). The Kubin and plate theories are based upon similar descriptions of packed beds, but the method of interpreting the chromatographic data is different for the two approaches.

The first objective of this work was to evaluate the Kubin theory for a nonadsorbable tracer by using experimental data for the helium (tracer)-nitrogen system. Data were also obtained for the slightly adsorbable system, nitrogen (tracer)-helium. By combining the results for the two systems, it is possible to estimate the rate of physical adsorption for nitrogen on silica gel.

THEORETICAL RESULTS

Kubin Theory

In this theory the moments of the chromatographic peak leaving the bed are related to the parameters describing the mass transfer processes, that is the axial dispersion coefficient E_A, external mass transfer coefficient k_A, intraparticle diffusivity D_e, and the adsorption rate constant k_{Ads}, at a site within the porous particle. The results for the first absolute and second central moments, which are developed elsewhere (*1, 2*), are

$$\mu_1' = \frac{L}{v}(1+\delta_0) + \frac{t_{0A}}{2} \tag{1}$$

$$\mu_2 = \frac{2L}{v}\left[\delta_1 + \frac{E_A}{\alpha}(1+\delta_0)^2\frac{1}{v^2}\right] + \frac{(t_{0A})^2}{12} \tag{2}$$

where

$$\delta_0 = \frac{1-\alpha}{\alpha}\beta\left(1+\frac{\rho_p K_A}{\beta}\right) \tag{3}$$

and

$$\delta_1 = \delta_a + \delta_i + \delta_e \tag{4}$$

with

$$\delta_a = \left(\frac{1-\alpha}{\alpha}\beta\right)\frac{\rho_p K_A^2}{k_{\text{Ads}}\,\beta} \tag{5}$$

$$\delta_i = \left(\frac{1-\alpha}{\alpha}\beta\right)\frac{R^2\beta}{15}\left(1+\rho_p\frac{K_A}{\beta}\right)^2\frac{1}{D_e} \tag{6}$$

$$\delta_e = \left(\frac{1-\alpha}{\alpha}\beta\right)\frac{R^2\beta}{15}\left(1+\rho_p\frac{K_A}{\beta}\right)^2\frac{5}{k_A R} \tag{7}$$

At the low flow rates reported here, the Nusselt number for external (fluid-to-particle) mass transfer is given by

$$N_{Nu} = 2 = \frac{k_A(2R)}{D_m} \tag{8}$$

where D_m is the molecular diffusivity. With this relationship, Equation (7) reduces to

$$\delta_e = \left(\frac{1-\alpha}{\alpha}\beta\right)\frac{R^2\beta}{15}\left(1+\rho_p\frac{K_A}{\beta}\right)^2\frac{5}{D_m} \tag{9}$$

At higher flow rates, when Equation (8) is not valid, the error introduced in replacing Equation (7) with (9) is usually low, because the contribution of external mass transfer resistance to the overall process is small (*4*). In other words, δ_e is small with respect to δ_a and δ_i. Note that δ_a represents the contribution of the adsorption rate at the site to the second moment, while δ_i is the contribution due to intraparticle diffusivity.

Equations (3), (5) to (7), and (9) apply for a pulse (square wave) of adsorbable tracer introduced into the feed. If a nonadsorbable tracer is used, $K_A = 0$, and these equations become

$$\delta_0 = \frac{1-\alpha}{\alpha}\beta \tag{3a}$$

$$\delta_a = 0 \tag{5a}$$

$$\delta_i = \left(\frac{1-\alpha}{\alpha}\beta\right)\left(\frac{R^2\beta}{15}\right)\frac{1}{D_e} \tag{6a}$$

$$\delta_e = \left(\frac{1-\alpha}{\alpha}\beta\right)\left(\frac{R^2\beta}{15}\right)\frac{5}{k_A R} \tag{7a}$$

and in place of Equation (9)

$$\delta_e = \left(\frac{1-\alpha}{\alpha}\beta\right)\left(\frac{R^2\beta}{15}\right)\frac{5}{D_m} \tag{9a}$$

The moments μ_1' and μ_2 can be evaluated from the observed chromatographic peaks for the tracer. Then the rate parameters are obtainable from Equations (1) to (6) and (9), or the simplified expressions for a nonadsorbable tracer.

EXPERIMENTAL PROCEDURE

When a nonadsorbable tracer is used, the retention time and second moment become much smaller than those for an adsorbable tracer. This reduces the accuracy of parameter determinations from the moments and increases the significance of entrance, exit, input pulse distortion, wall, and other side effects. All of these effects will be referred to hereafter as *entrance* and *exit* effects. For our experimental conditions, the retention time was of the order of 1 min.

The bed consisted of a 98 cm. length of silica gel particles packed in 0.200 in. I.D. copper tubbing. The properties of the silica are shown in Table 1. Three average particle sizes were studied. The mean particle sizes and void fractions in the bed were

Average particle size, cm.	Void fraction, α
0.050	0.376
0.0359	0.395
0.0227	0.405

The expected, slight decrease in void fraction with decrease in particle size was not observed. This is apparently because there was a wider distribution of sizes about the average for the large particles than for the small ones. This resulted in a better accommodation of particles in the bed, and lower void fraction, for the larger particles. All measurements were made at 75°C. and approximately 1 atm. pressure.

A pulse of tracer was introduced to the bed through a 0.25 cc. sample loop. With the flow rates employed (10 to 40 cc./min. at 75°C., 1 atm.), the sample injection time ranged from 0.00625 to 0.025 min. It was found that nitrogen was slightly adsorbed on the gel so that data suitable for application of the nonadsorbable gas equations were obtained by using helium as a tracer in a stream of nitrogen. Runs were also made with nitrogen as a tracer.

The experimental equipment and procedure was similar to that described in reference 4. The carrier gas passed through the reference side of the thermal conductivity cell detector, then through the column, and returned through the sample side of the cell. An aerograph with a recorder were used. Precautions already described (*4*) were taken to ensure reliable data. The beds were pretreated by maintaining them at 200°C. for 18 hr., while carrier gas flowed through at a rate of 5 to 10 cc./min. Runs were made at different flow rates for each particle size. The chromatographic peaks were recorded and the moments evaluated from the peak height by the Gaussian approximation (*12*). A comparison of this approximate result with the proper integrations by using the whole curve indicated a difference of but a few percent.

A set of blank runs were made at various flow rates, with nitrogen as tracer, to establish the contribution of entrance and exit connections to the second moment. For these runs, the packed columns were replaced with a short length of 0.065 in. I.D. copper tubing having a volume less than 0.5 cc. Earlier experiments (*4*) established that the deviations of the input pulse from a square wave and the length of 0.065 in. tubing gave negligible contributions to the second moment.

TABLE 1. PROPERTIES OF SILICA GEL PARTICLES*

Surface area (from low temp. N_2 adsorption)	832 sq.m./g.
Void volume	0.43 cc./g.
Particle density	$\rho_p = 1.13$ g./cc.
Internal void fraction	$\beta = 0.486$
Average pore radius ($2V_g/S_g$)	11Å

* Grade 05 of the Davison Chemical Division, Grace Co. properties supplied by manufacturer.

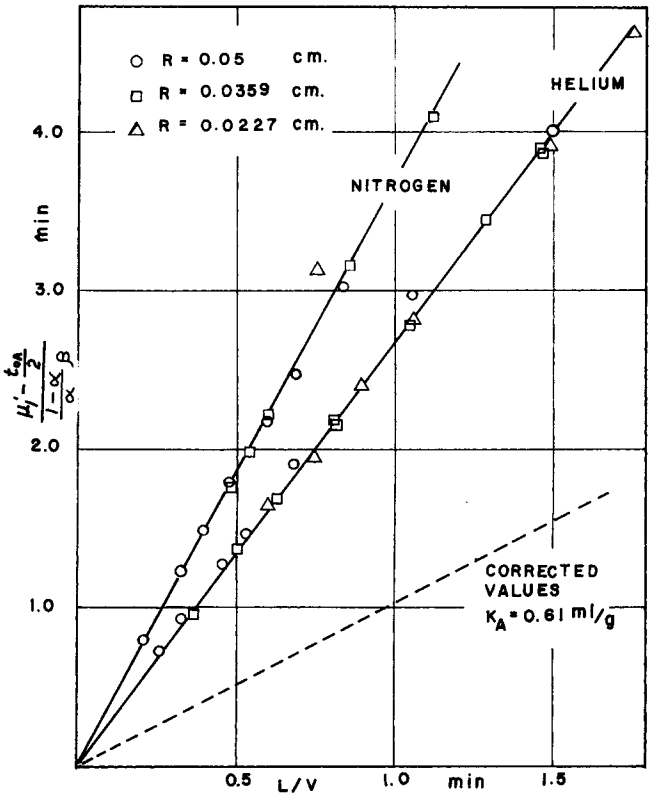

Fig. 1. First moments for nitrogen and helium.

RESULTS

Analysis of First Moments

For a nonadsorbable, or slightly adsorbable, gas, the second moments are small enough that accurate evaluation of the contribution of entrance and exit effects to μ_2 is necessary. For adsorbable tracers, such blank runs are not required. This procedure would normally be necessary also for first moments. However, in our case no blank runs (in which the bed was replaced by an empty tubing) were needed, because the runs for the bed, with helium as a tracer, could be used for this purpose. By taking $K_A = 0$ for helium, Equations (1) and (3) become

$$\mu_1' = \frac{L}{v}\left(1 + \frac{1-\alpha}{\alpha}\beta\right) + \frac{t_{0A}}{2}$$

This does not include a contribution for entrance and exit effects. If $(\mu_1')_e$ represents this contribution, the equation is

$$(\mu_1')_{He} = \frac{L}{v}\left(1 + \frac{1-\alpha}{\alpha}\beta\right) + (\mu_1')_e + \frac{t_{0A}}{2} \quad (10)$$

By taking $(\mu_1')_e$ the same for a slightly adsorbable gas, Equations (1) and (3) written to include entrance and exit effects give

$$(\mu_1')_{N_2} = \frac{L}{v}\left(1 + \frac{1-\alpha}{\alpha}\beta\right) + \frac{L}{v}\left(\frac{1-\alpha}{\alpha}\beta\right)\frac{\rho_p K_A}{\beta} + (\mu_1')_e + \frac{t_{0A}}{2} \quad (11)$$

Now, Equation (10) can be subtracted from (11) to eliminate $(\mu_1')_e$:

$$\frac{(\mu_1')_{N_2} - (\mu_1')_{He}}{\frac{1-\alpha}{\alpha}\beta} = \frac{L}{v}\left(\frac{\rho_p K_A}{\beta}\right) \quad (12)$$

Table 2. Axial Dispersion Results

Tracer	D_m, sq.cm./sec.	$R = 0.05$ cm. E_A, sq.cm./sec.	q_{ext}	$R = 0.0359$ cm. E_A, sq.cm./sec.	q_{ext}	$R = 0.0277$ cm. E_A, sq.cm./sec.	q_{ext}
Helium	0.88	0.321	1.03	0.302	1.15	0.243	1.45
Nitrogen	0.88	0.241	1.36	0.241	1.44	0.239	1.49

Average $q_{ext} = 1.43$ for N_2
$= 1.21$ for He

By plotting the difference between the first moments, in the form suggested by Equation (12), the effect of entrance and exit effects is eliminated. This difference gives an accurate value for the first moment of the slightly adsorbable gas. Figure 1 shows both the individual data for nitrogen and helium and also the difference (the dotted line). The results are linear in L/v for both nitrogen and helium, as predicted by Equations (11) and (10). The value of K_A for nitrogen obtained from slope of the dotted line, by using Equation (12), is 0.61 cc./g.

No information was found in the literature on adsorption equilibrium data for nitrogen on silica gel at 75°C. However, Homfray (*13*) reported K_A values of 30,600, 3,100, and 145 cc./g. at 83°, 195°, and 273°K., respectively, for nitrogen on wood charcoal. Extrapolating these results to 75°C. is uncertain, but a value between 0 and 10 cc./g. is estimated for this different adsorbant. For silica gel of unknown properties, K_A values for ammonia have been reported (*14*) as 53.5 and 23.0 cc./g. at 313° and 373°K. For sulfur dioxide, the results were 9.75 and 1.12 cc./g. These data would suggest that K_A for nitrogen would be somewhat smaller but probably within one order of magnitude of that for sulfur dioxide. This is in general agreement with our value of 0.61 cc./g. Using the silica whose properties are given in Table 1, Schneider and Smith (*5*) obtained, for 75°C., $K_A = 130$ cc./g. for *n*-butane, 32 for propane, and 10 for ethane.

Analysis of Second Moments

Figure 2 shows the second moments for helium (for $R = 0.05$ mm.), for the blank runs, and also the corrected results (dotted line). The correction was made by subtracting the value of $\mu_2 - t_{0A}^2/12$ for a blank run from the packed bed value, at the same flow rate. Similar corrections were made for the other particle sizes and for the data with nitrogen as tracer. The corrected results are plotted in Figures 3 and 4. Straight lines are drawn through the points, in accordance with the linear form suggested by rearrangement of Equation (2):

$$\frac{\mu_2 - t_{0A}^2/12}{2\,\frac{L}{v}} = \delta_1 + \frac{E_A}{\alpha}(1 + \delta_0)^2 \frac{1}{v^2} \qquad (2a)$$

From the slopes of these lines, E_A was evaluated. For helium, Equation (3*a*) was used for δ_0, while for the slightly adsorbable nitrogen, Equation (3) was employed with $K_A = 0.61$ cc./g. Perhaps the most meaningful interpretation of axial dispersion is through the external tortuosity factor, defined in terms of E_A as follows:

$$E_A = \frac{\alpha\, D_m}{q_{ext}} \qquad (13)$$

Tortuosity factors should be independent of the diffusing gas and are a measure of the length of the diffusion path with respect to the length of the column. For an ideal diagonal path, $q_{ext} = \sqrt{2}$. The nitrogen data in Table 2 give 1.43 and the helium data 1.21. For columns prepared from the same type of silica gel particles, Schneider and Smith (*4*) obtained 1.35 and Cerro and Smith (*6*) 1.54. All of these data are close to the expected result. The helium results are low, perhaps because of the lower

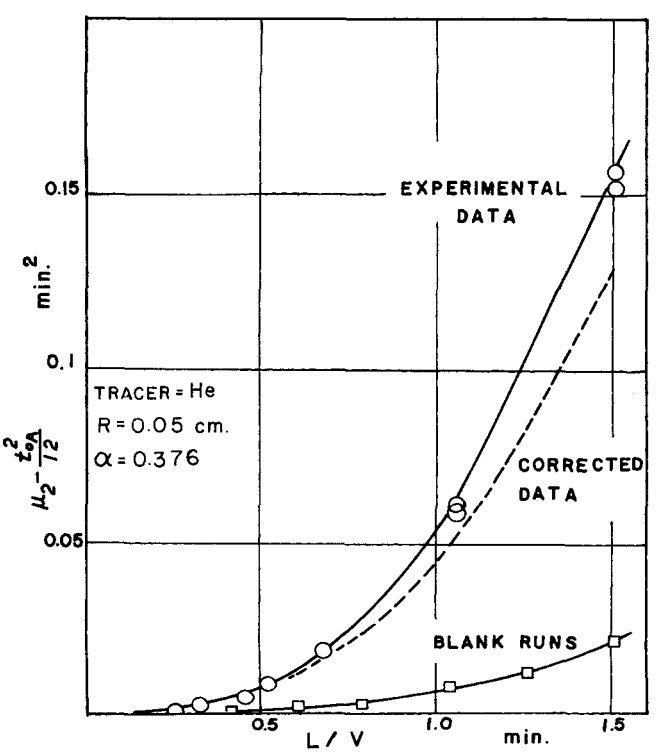

Fig. 2. Second moments for helium.

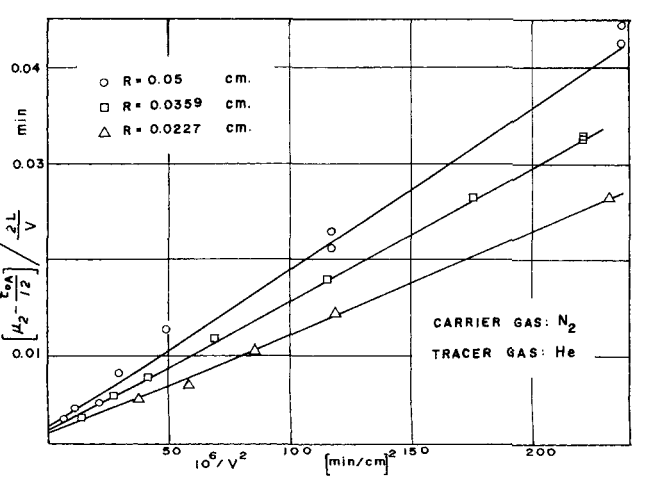

Fig. 3. Second moment function for helium.

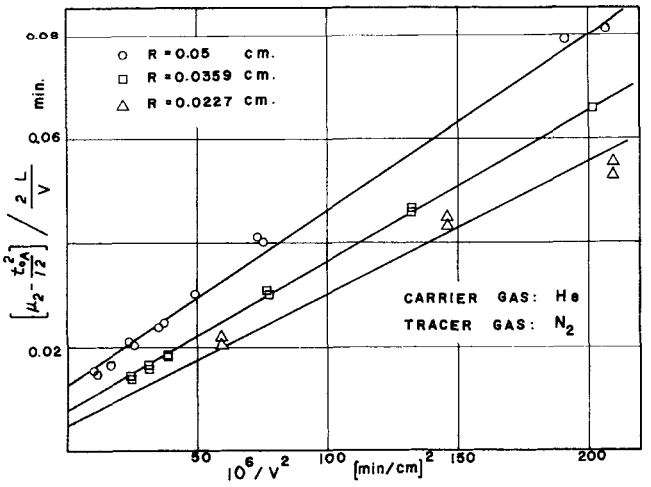

Fig. 4. Second moment function for nitrogen.

level of the second moments (compare Figures 3 and 4) which makes absolute experimental errors more significant.

The ordinate at nearly any velocity in Figure 3 is larger than the intercept. This shows that, for nonadsorbable gases, the contribution of axial dispersion to the second moment is larger than the contributions due to external diffusion, intraparticle diffusion, and adsorption on the pore surface. This explains why accurate results for E_A were obtained and suggests that the results for the other parameters may be less satisfactory with the helium data. The data apply to beds of relatively small particles. The intercept could be made relatively larger by using larger particles, which would in turn necessitate a larger column diameter.

The intercepts in Figures 3 and 4 are equal to δ_1. The derived expressions for δ_1 are obtained from Equations (6*a*) and (9*a*) for helium, and Equations (5) to (7) for nitrogen:

$$(\delta_1)_{He} = \left(\frac{1-\alpha}{\alpha}\beta\right)\frac{R^2\beta}{15}\left(\frac{1}{D_e}+\frac{5}{D_m}\right) \qquad (14)$$

$$(\delta_1)_{N_2} = \left(\frac{1-\alpha}{\alpha}\beta\right)\left[\frac{\rho_p K_A^2}{k_{Ads}\beta}+\frac{R^2\beta}{15}\left(1+\rho_p\frac{K_A}{\beta}\right)^2\left(\frac{1}{D_e}+\frac{5}{D_m}\right)\right] \qquad (15)$$

These expressions show that a linear relationship should result when the intercepts are plotted vs. R^2. Figure 5 is such a plot. Equation (14) further indicates that the intercept for helium should be zero, while the data in Figure 5 suggest a finite intercept. The helium moments are so low that even the different connections used for the blank runs can give erroneous values for the entrance and exit effects in the packed bed. Also, blank runs will not account for input pulse distortion and similar effects which we have included in the entrance and exit category. It is believed that this is the explanation for the small but finite intercept in Figure 5. However, the intercepts do not affect the calculation of the intraparticle diffusivity. This quantity, as seen from Equations (14) and (15), depends upon the slopes of the lines in Figure 5. The resulting values for D_e are given in Table 3 along with internal tortuosities, q_{int}, calculated from the expression

$$D_e = \frac{D_K\beta}{q_{int}} \qquad (16)$$

The Knudsen diffusivity is used here because the mean pore radius (11Å from Table 1) is much less than the mean free path of either nitrogen or helium at 75°C. and 1 atm. Internal tortuosities should be independent of the diffusing gas and be characteristic of the geometry of the porous material. The difference between the helium and nitrogen values in Table 3 is believed to be due again to the small magnitude of δ_1, that is, the very small contributions of intraparticle diffusion and external diffusion to the second moment of a nonadsorbable gas. Schneider and Smith (*4*) obtained 3.35 for q_{int} for the same silica gel by an independent method. Their value was obtained by measuring q_{int} with ethane as a tracer at successively higher temperatures until surface diffusion was eliminated. The concurrence of the nitrogen value in Table 3 with this result lends confidence to a value of about 3.4 for this silica.

At the operating conditions used here, measurements with a nonadsorbable tracer give but approximate results for the intraparticle diffusivity. The magnitude of δ_1, and the accuracy of the resulting D_e, could be increased by using larger particles packed in a tube of larger diameter. This was recognized by Davis and Scott (*10*) who used ⅛- to ½-in. particles in appropriately sized tubes. Measurements for one particle size are sufficient to establish K_A, E_A, D_e, and k_{Ads}. Thus, Equation (2) for the second moment could be applied to a series of μ_2 vs. velocity data to evaluate the four parameters. A minimum of four velocities would be needed, and additional points would improve the accuracy of the results. Actually, data for different particle sizes are particularly helpful for establishing D_e because the contribution to μ_2 of intraparticle diffusion resistance is proportional to the square of the particle

Table 3. Intraparticle Diffusion Results

Tracer	Helium	Nitrogen
D_K, sq.cm./sec.	9.97×10^{-3}	3.77×10^{-3}
D_e, sq.cm./sec.	9.4×10^{-4}	5.3×10^{-4}
q_{int}	5.2	3.4

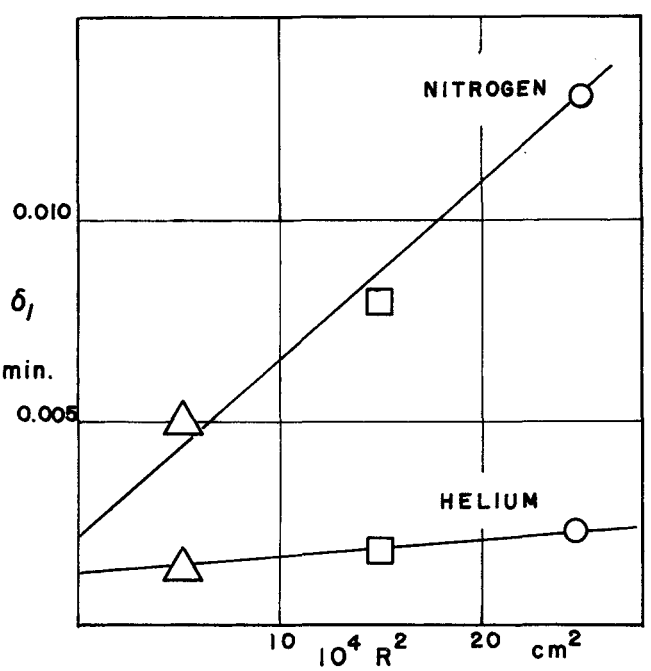

Fig. 5. δ_1 vs. R^2 for nitrogen and helium.

radius. When such information is available, the parameters may be determined either graphically, as illustrated in this paper, or by statistical methods by using Equation (2).

Adsorption Rate Constant for Nitrogen

The rate of adsorption of slightly adsorbable gases is difficult to measure by standard methods. Without additional information, the chromatographic data only for the gas in question would also not be useful for this purpose. This is illustrated in Figure 5. The intercept for nitrogen is so small that it is of the same order as uncertainties, such as those due to entrance and exit effects, in the experimental results. However, runs at the same operating conditions with a nonadsorbable gas would be expected to involve the same uncertainties. According to this interpretation, the true intercept for nitrogen data is the difference between the observed values of δ_1 for nitrogen and helium. Then, according to Equation (15)

$$(\delta_1)_{N_2,corr} = (\delta_1)_{N_2,obs} - (\delta_1)_{He,obs} = \frac{\rho_p K_A^2}{k_{Ads}} \left(\frac{1-\alpha}{\alpha} \right) \tag{17}$$

From the intercepts in Figure 5, $k_{Ads} = 13.4$ cc./(g.)(sec.) for nitrogen at 75°C. There appear to be no data in the literature for comparison with this result. Rate of adsorption data commonly available include unknown effects due to intraparticle diffusion and external mass transfer. The rate constant calculated from the collision frequency by using kinetic theory is many orders of magnitude high, because the condensation coefficient for nitrogen at 75°C. should be very low; also, this coefficient is not known. Schneider and Smith (4) for the same silica found k_{Ads} to be 1,500, 255, and 167 cc./(g.)(sec.) for *n*-butane, propane, and ethane, respectively, at 50°C. Since nitrogen has a lower boiling point than that of ethane, 13.4 for nitrogen at 75°C. is not unreasonable, but a more quantitative comparison cannot be made. It should be noted that these constants all refer to a linear rate equation, rate = $k_{Ads}(C)$, applicable only at low surface coverages.

CONCLUSIONS

The Kubin theory can be used to obtain accurate intraparticle and external mass transfer rate parameters for adsorbable or slightly adsorbable gases. Small particle sizes and relatively short bed lengths are satisfactory. For adsorbable gases, entrance and exit effects can be neglected safely, but for slightly adsorbable tracers, corrections are required.

To determine intraparticle diffusivities accurately with a nonadsorbable tracer, long beds of relatively large particles should be used. However, runs with a nonadsorbable gas can be used effectively to correct the results for a slightly adsorbable gas. In particular, the second moments can be corrected so that an estimate can be made for the adsorption rate constant for a slightly adsorbable substance.

ACKNOWLEDGMENT

The financial assistance of the National Science Foundation, Grant No. GP 2990, is gratefully acknowledged.

NOTATION

C = gas concentration, g. moles/cc.
D_e = effective, intraparticle diffusivity, sq.cm./sec.
D_K = Knudsen diffusivity, sq.cm./sec.
D_m = binary molecular diffusivity, sq.cm./sec.
d_p = average particle diameter, cm.
E_A = axial dispersion coefficient, sq.cm./sec.
K_A = adsorption equilibrium constant for tracer, cc./g.
k_{Ads} = adsorption rate constant on pore surface, cc./(g.)(sec.)
k_A = fluid-particle mass transfer coefficient, cm./sec.
L = bed length, cm.
N_{Nu} = Nusselt number for external mass transfer
q = tortuosity factor; q_{ext} applies to path of fluid in packed bed, q_{int} = intraparticle tortuosity
R = average radius of particle, cm.
t_{0A} = injection time of tracer, min.
v = linear velocity of the carrier gas in the interparticle space, cm./min.

Greek Letters

α = void fraction in bed
β = intraparticle void fraction
δ_0 = coefficient defined by Equation (1)
δ_1 = contribution to second moment function, defined by Equation (2), sec.
δ_a = contribution of surface adsorption to second moment function, Equation (5), sec.
δ_i = contribution of intraparticle diffusion to second moment function, Equation (6)
δ_e = contribution of external diffusion to second moment function, Equation (7)
μ_1' = first absolute moment of chromatographic peak, sec.
$(\mu_1')_e$ = entrance and exit contributions to first absolute moment, sec.
μ_2 = second central moment, sec.^{2}
ρ_p = density of silica gel particles, g./cc.

Subscripts

corr = corrected
obs = observed

Note

Moments are reported on the basis of measuring time in minutes, while the rate parameters and equations from which they are calculated are based upon time in seconds.

LITERATURE CITED

1. Kubin, M., *Collection Czech. Chem. Commun.*, **30**, 1104 (1965).
2. *Ibid.*, 2900.
3. Kucera, E., *J. Chromatog.*, **19**, 237 (1965).
4. Schneider, Peter and J. M. Smith, *AIChE J.*, **14**, 762 (1968).
5. *Ibid.*, 886.
6. Cerro, R. L., and J. M. Smith, *Ind. Eng. Chem. Fundamentals*, **8**, 796 (1969).
7. Martin, A. J. P., and R. L. M. Synge, *Biochem J.*, **35**, 1359 (1941).
8. Glueckauf, E., *Disc. Faraday Soc.*, **7**, 12 (1949).
9. van Deemter, J. J., F. J. Zuiderweg, and A. Klinkenberg, *Chem. Eng. Sci.*, **5**, 271 (1956).
10. Davis, B. R., and D. S. Scott, IV International Congress on Catalysis. Symposium III. Paper No. 13, Novosibirsk (1968).
11. Giddings, J. Calvin, "Dynamics of Chromatography," Part I., Chapt. 4, Dekker, New York (1965).
12. Klinkenberg, A., and F. Sjenitzer, *Chem. Eng. Sci.*, **5**, 258 (1956).
13. Homfray, C., *Z. Physik. Chem.*, **121**, 1525 (1922).
14. Davidheiser, L. Y., and W. A. Patrick, *J. Am. Chem. Soc.*, **44**, 1 (1922).

Manuscript received January 6, 1969; revision received May 5, 1969; paper accepted May 7, 1969.